Materials Advances

ROYAL SOCIETY OF CHEMISTRY

PAPER

View Article Online
View Journal | View Issue

Cite this: *Mater. Adv.*, 2025, **6**, 5196

Efficient and selective *N*-benzylation of amines using Pd-doped La-BDC MOF†

Amreet Kaur,[a] Yadvinder Singh,[b] Avtar Singh,[cd] Sandeep Kaushal*[e] and Rahul Badru*[a]

Received 16th April 2025,
Accepted 16th June 2025

DOI: 10.1039/d5ma00372e

rsc.li/materials-advances

Transition metal catalysis has become increasingly important in direct *N*-alkylation *via* the hydrogen borrowing mechanism, an environmentally friendly pathway that produces only water as a by-product. However, the application of inner-transition metal catalysts for the alkylation of amines has been explored on a limited scale. Herein, we investigate the potential of a Pd-doped La-BDC (benzene-1,4-dicarboxylate, terephthalic acid) MOF in the *N*-benzylation of amine substrates. The isolation of imine and benzaldehyde intermediates confirms that the reaction follows a hydrogen auto-transfer pathway. Reaction conditions, including temperature, reaction time, and catalyst loading, were optimized to achieve high conversion and selectivity. Extensive characterization using FTIR, FESEM, HRTEM, EDS, XPS, and nitrogen adsorption–desorption measurements assessed the structural and textural properties of the synthesized Pd@La-BDC MOF. Compared to previous literature, our findings provide valuable insights into the application of La-derived MOFs in sustainable catalysis and offer new possibilities for synthesizing *N*-benzylated products using benzyl alcohol as an alkylating agent.

1. Introduction

The relentless pursuit to improve and simplify chemical reactions is paramount, especially with the goal of eliminating hazardous chemicals while achieving high yields. This endeavor to develop safer and more sustainable chemical processes is vital for advancing science, biology, and materials science, ultimately benefiting humanity through the principles of green chemistry. Such research and technological advancements are critical for the growth of various scientific domains, fostering the creation of processes that significantly contribute to environmental preservation and human well-being.

The usage of dimethyl carbonates and alcohols as alkylating agents has gained attention in the past two decades due to their environmentally friendly nature. These methods align with green chemistry principles by reducing hazardous waste and improving the overall sustainability of chemical processes. For example, the use of dimethyl carbonate and alcohols in *N*-alkylation reactions has been shown to produce minimal by-products and operate under milder conditions, making it a preferred choice for sustainable synthesis.[1–3] Among these two modes, the *N*-alkylations with dialkylcarbonates generate alcohols as the byproduct, whereas water is the only side product of the reaction among amines and alcohols. Additionally, *N*-alkylation with dialkylcarbonates has always suffered from selectivity issues as it generates a mixture of alkylated and carboxymethylated products, as reflected in the tremendous work reported with them.[4,5] They have also been reported to deliver over-alkylated products due to dialkylation or methylation of the activated CH_2 group in addition to the normal amine functionality. *N*-Alkylation with alcohols thus remains the preferred approach among all other documented methods.[6,7] *N*-Alkylation with alcohols follows hydrogen borrowing methodology (Scheme 1), wherein the transition metal catalysts are involved in hydrogen auto-transfer with the amine substrate, generating aldehydes which then condense with an amine to liberate an imine, which is reduced to an alkylated amine by back H-transfer.[2,3] This technique has become popular and stands out of all methodologies as it's a quicker way of accessing C–C and C–N bond formulations in a one-pot sustainable mode avoiding the need for separation and purification of any intermediates. Moreover, this technique avoids the need for specialized conditions or pre-functionalized substrates.

[a] *Department of Chemistry, Sri Guru Granth Sahib World University, Fatehgarh Sahib, Punjab, India. E-mail: rahulbadru@gmail.com*
[b] *Department of Botany, Central University of Punjab, Bathinda-151401, Punjab, India*
[c] *Department of Chemistry, School of Science, Navajo Technical University, Crownpoint, NM, 87313, USA*
[d] *Department of Chemistry, Sri Guru Teg Bahadur Khalsa College, Anandpur Sahib-140118, Punjab, India*
[e] *Regional Institute of Education, NCERT, Ajmer, Rajasthan, India. E-mail: kaushalsandeep33@gmal.com*

† Electronic supplementary information (ESI) available. See DOI: https://doi.org/10.1039/d5ma00372e

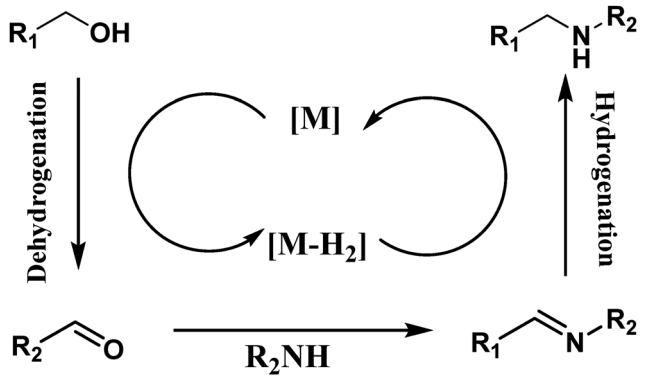

Scheme 1 The metal-catalyzed amination reaction: the hydrogen borrowing mechanism in general.

Much research has been conducted previously to investigate the use of various transition metal (Rh, Ru, Mn, Co, Pd, Ir)-based catalysts in *N*-alkylations *via* hydrogen auto-transfer.[8–13] There have also been numerous reports on the use of tandem catalysts in these reactions, involving transition metal combination in the same catalyst.[14,15] Aside from these, metal–organic frameworks (MOFs) or supported MOF systems have been used to achieve *N*-alkylation with alcohols as alkylating agents.[15,16]

MOFs have served as versatile efficient catalysts in a number of organic transformations, owing to their tunable pore size and high surface area to volume ratio. The MOFs are insoluble in most organic solvents and thus the easy post-process separation adds on to their importance as heterogenous catalysts. Although their catalytic potential has been extensively established in a number of other organic synthesis processes, their utilization in *N*-alkylation with alcohols is only partially studied.[15–18,34] Although a high efficiency and selectivity have been achieved with these protocols, all of these processes suffer from one or more drawbacks, including the use of expensive non-recoverable catalysts, limited substrate scope, need for co-catalysts, ligands or bases and a high time interval.

To the best of our knowledge, reports on inner transition metal-based catalysts for *N*-alkylation of amines are minimal,[17,18] and our comparative analysis with these limited studies highlights the distinctiveness of our results. So, in order to address this and to fulfil our continued interest in developing effective and sustainable methodologies for organic transformations,[19–23] we hereby report the application of a Pd-incorporated La-BDC MOF as a catalyst in the *N*-benzylation of amines, avoiding the use of hydrogen, organic ligands and high-pressure conditions. With the present methodology, it is possible to selectively and efficiently benzylate a variety of aromatic amine substrates with benzyl alcohol without isolating any poly-alkylation products. The reaction conditions are benign in comparison to previous methodologies. The reusability and stability of the MOF catalyst in the executed reaction conditions have also been examined, which adds onto the sustainability of the protocol. Interestingly, mechanistic details have been established based on products and intermediates isolated while assessing the reaction profile on a time scale using gas chromatography. The reaction has been found to follow the hydrogen auto-transfer mechanism.

2. Experimental

2.1. Representative procedure for La-BDC MOF synthesis

The solvothermal method has been employed to synthesize La-BDC MOF, similar to the one reported in the literature.[24] In a 30 mL 1 : 1 water–DMF mixture, 10 mmol each of the salts lanthanum nitrate and BDC were dissolved and the whole mixture was moved to a 150 mL Teflon-lined autoclave and kept at 120 °C in a pre-heated oven for 24 h. The contents were then allowed to cool to room temperature, and the MOF precipitated out. The solid thus obtained was filtered and washed with distilled water. Before being used, the filtered solid was activated for 4 hours by placing it in a vacuum oven maintained at 100 °C.

2.2. Representative procedure for Pd-supported La-BDC MOF synthesis

To prepare a Pd-loaded MOF, 5 mg of palladium nitrate was loaded into a pre-formed solution containing 100 mg of La-BDC MOF in 40 mL of ethanol. The *in situ* reduction of palladium ions was done by the addition of a 10% solution of sodium borohydride in water. The mixture was stirred continuously using a magnetic stirrer for 1 h for reduction to complete the reaction. The Pd-loaded MOF thus obtained was filtered off from the solution and washed with 20 mL ethanol and 20 mL water. The isolated solid Pd@La-BDC MOF was dried in a vacuum oven at 100 °C for 24 hours.

2.3. Representative procedure for the catalytic *N*-benzylation reaction

The *N*-benzylation reactions were carried out under autoclave conditions. The Teflon tube was charged with 10 mmol of amine, 50 mmol benzyl alcohol, 10 mL toluene and 5 mol% of MOF catalyst. The Teflon tube was sealed with Teflon tape before being immersed into a preheated furnace. After commencement of time, the reaction mixture was cooled and the heterogenous catalyst was filtered off. The percentage yields of all the products were ascertained using GC analysis and adding *n*-hexadecane as the internal standard. After completion of the reaction, 20 mL of *n*-hexadecane was added to the reaction mixture, which was diluted with ethyl acetate and subjected to filtration over a plug of silica and then analysed with GC. All the products were obtained over a silica gel column eluted with a hexane–ethyl acetate mixture.

2.4. Kinetic study for the *N*-benzylation of aniline

The kinetic studies were carried out in a glass reactor equipped with a magnetic stirrer. To establish the reaction kinetics, varying amounts of benzyl alcohol (0.1–0.4 mol) and aniline (0.1–0.4 mol) in toluene were made to react at 150 °C (while varying only one reactant at a time), with 5 mol% of MOF

catalyst. *n*-Hexadecane (0.2 mmol) was added as an internal standard. At different intervals, about 50 μL aliquots were withdrawn. Each aliquot was diluted with ethyl acetate before being centrifuged, and the supernatant thus isolated was examined on a gas chromatogram.

3. Results and discussion

3.1. Pd@Al-BDC MOF characterization

3.1.1. Fourier transform infrared spectroscopy (FTIR) analysis. The FTIR examination of the MOF sample predicts ligand coordination to the metal atom as evidenced by peak shifting of

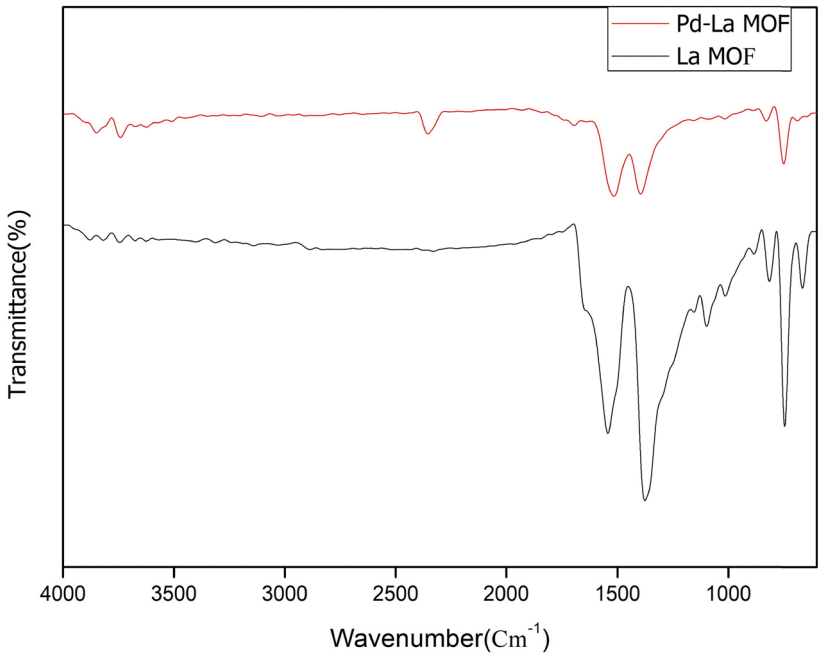

Fig. 1 FTIR spectra of the synthesized Pd@La-BDC and La-BDC MOFs; the spectra reveal shifts in the carboxylate and M–O bond vibrations upon Pd incorporation into La-BDC, confirming successful synthesis and structural modification of the Pd@La-BDC MOF.

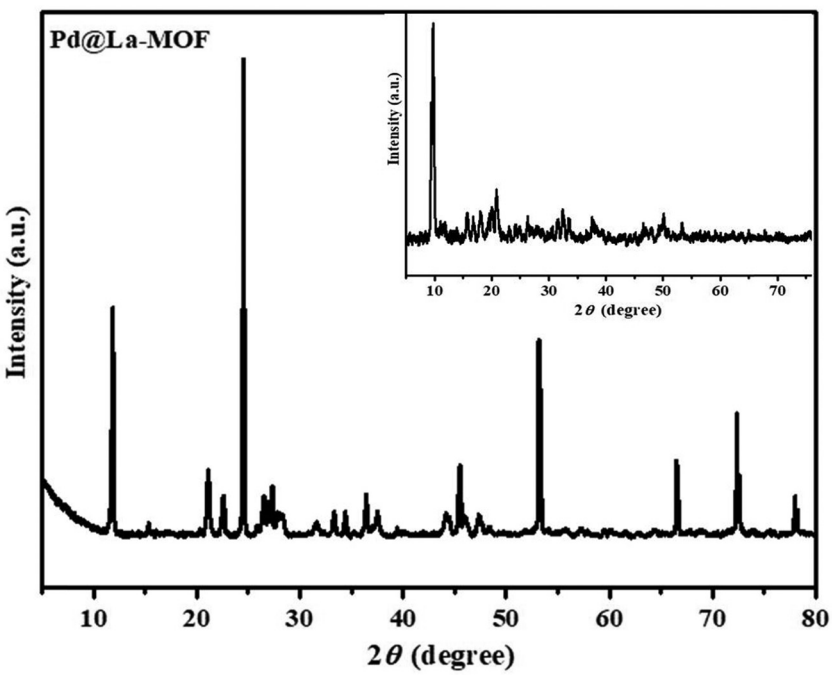

Fig. 2 X-ray diffraction (XRD) pattern of the Pd@La-BDC MOF nanocomposite (inset: La-BDC MOF); the XRD pattern confirms the crystalline structure and successful incorporation of Pd into the La-BDC MOF, with well-defined peaks indicating maintained structural integrity and phase purity.

the ligand's typical stretchings. Fig. 1 illustrates the FTIR spectra of the Pd@La-BDC and La-BDC MOFs. The M–O stretching, carbonyl stretching of the carboxylate and aromatic C=C bond stretching appeared at 694 cm^{-1}, 1570 cm^{-1}, 1380 and 1100 cm^{-1} in the FTIR spectra recorded for the La-BDC MOF. A slight peak shifting of carboxylate stretching and M–O stretching was observed in the FTIR spectra of the Pd@La-BDC MOF. The M–O peak shifted to 680 cm^{-1} and the new carboxylate stretchings were shifted towards a lower wavenumber of 1515 cm^{-1}.

3.1.2. X-ray diffraction (XRD) analysis. XRD patterns of the as-synthesized La-MOF and Pd@La-BDC MOF nanocomposites are given in Fig. 2. The XRD pattern of La-MOF displays (Fig. 2 inset) many small distinct diffraction peaks at 2θ = 9.5°, 14.5°, 16.6°, 30.6°, and 33.4° with *d*-spacings of 8.9, 6.09, 5.3, 2.9, and 2.6 Å, respectively. This XRD pattern of the La-MOF specifies the crystalline nature of the MOF structure and is appropriate with the JCPDS Card number 96-720-4706. Furthermore, after the loading of Pd metal into the La-MOF, the XRD patterns of the Pd@La-BDC MOF nanocomposite show diffraction peaks at 2θ = 40.1° and 46.7° well matched with JCPDS no. 46-1043 and revealing that the crystallinity of the as-prepared MOF has increased and also confirmed the presence of Pd nanoparticles in the MOF.[25]

3.1.3. Surface studies. The surface morphologies of the synthesized La-BDC MOF and Pd@La-BDC MOF nanocomposites were discovered by recording their FESEM images. Fig. 3a confirms that the La-MOF has a distorted spherical shape. Whereas, the morphology of the Pd@La-BDC MOF nanocomposite has developed a sheet like structure with deposition of Pd on the surface of the sheets (Fig. 3b–f). An energy-dispersive spectroscopic (EDS) and element mapping investigation were carried out to determine the elemental composition of the Pd@La-BDC MOF nanocomposite (Fig. 3g) which indicated that uniformly dispersed Pd, La, O and C elements are present in the nanocomposite.

3.1.4. High resolution transmission electron microscopy. High-resolution transmission electron microscopy (HRTEM)

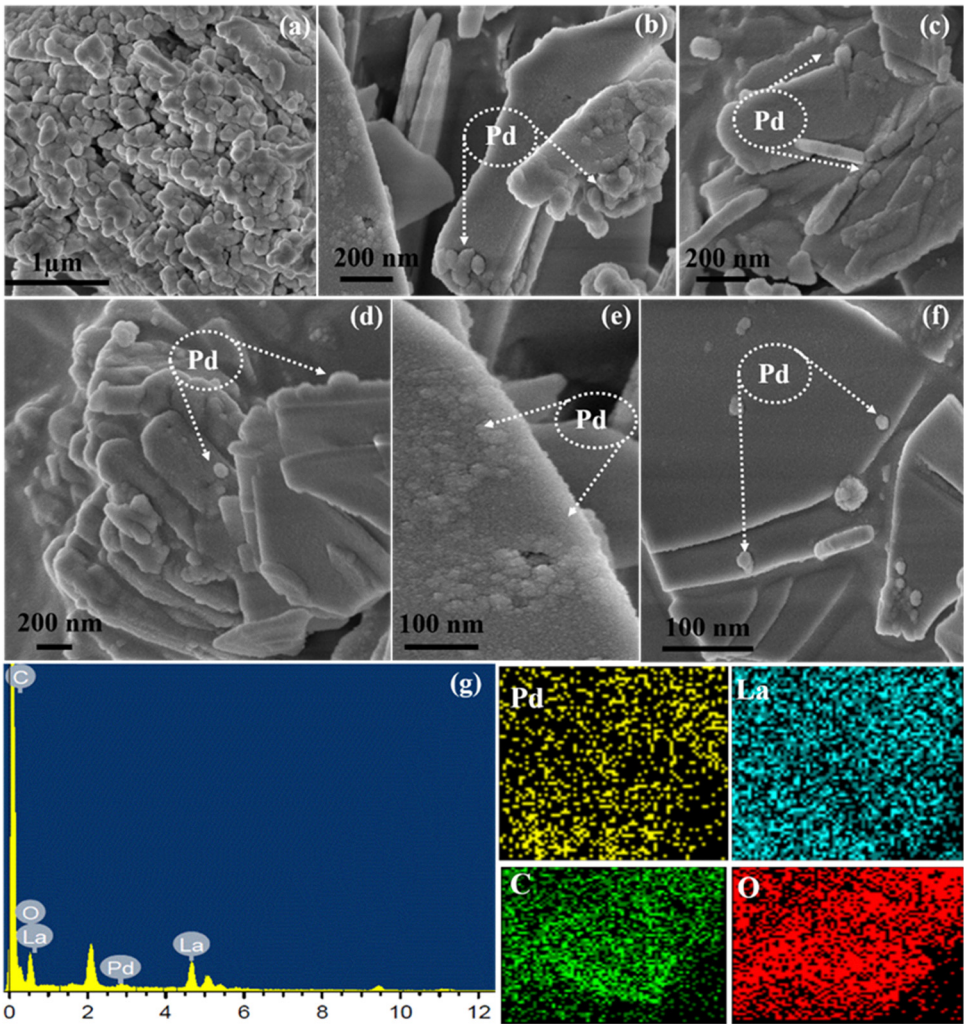

Fig. 3 (a) The FESEM image of the pristine La-BDC MOF shows a uniform morphology; (b)–(f) FESEM images of the Pd@La-BDC MOF nanocomposite illustrate successful Pd incorporation, with morphological changes; (g) EDS analysis confirms the presence and uniform distribution of Pd and other constituent elements in the nanocomposite.

observations were conducted to investigate the morphology and structure of the Pd@La-BDC MOF nanocomposite (Fig. 4a–e). The HRTEM images revealed that the synthesized Pd@La-MOF exhibits a distinct 2D sheet-like structure. Fig. 4f shows an exceptionally aligned crystal structure with an interplanar spacing of 0.29 nm. Furthermore, the selected area electron diffraction (SAED) pattern indicated the polycrystalline nature of the Pd@La-BDC MOF nanocomposite (Fig. 4g), suggesting

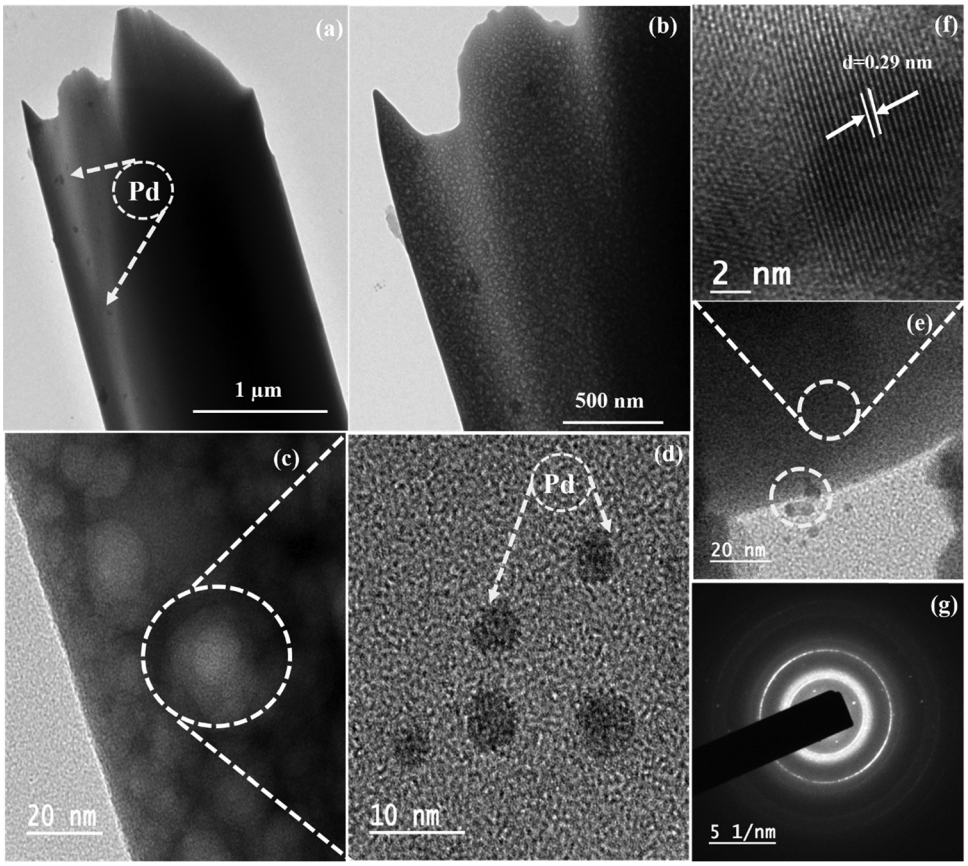

Fig. 4 (a)–(e) High-resolution transmission electron microscopy (HRTEM) images display the homogeneous distribution of palladium (Pd) within the Pd@La-BDC MOF nanocomposite, highlighting the consistent integration of Pd across the material; (f) interplanar spacing; (g) the selected area electron diffraction (SAED) pattern confirms the well-defined crystalline structure of the Pd@La-BDC MOF nanocomposite.

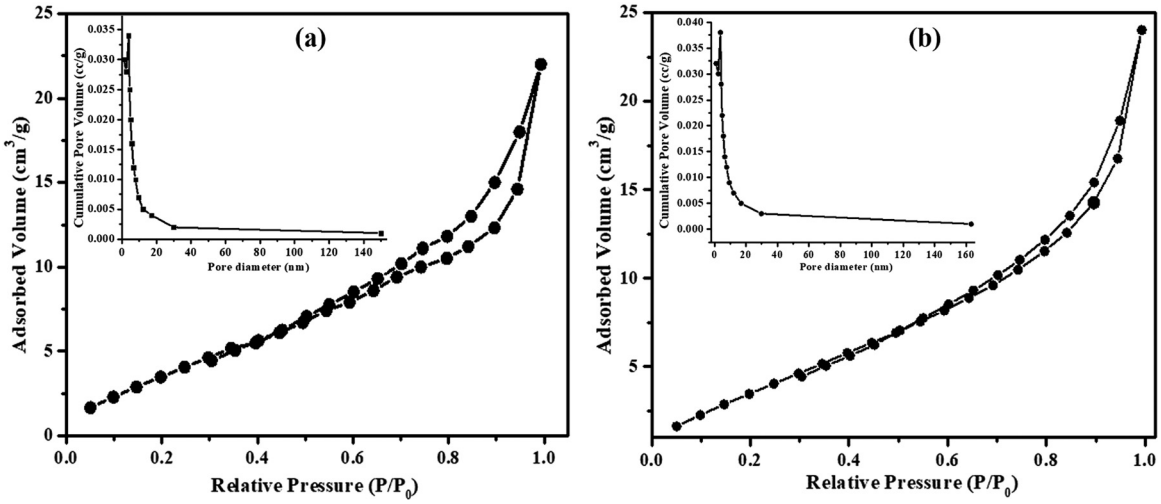

Fig. 5 N_2 adsorption–desorption isotherms of the (a) La-BDC MOF and (b) Pd@La-BDC MOF nanocomposite, with the inset showing pore size distribution, demonstrating the material's high surface area and porosity.

the presence of multiple crystalline domains within the material. The significance of these findings lies in the potential applications of the Pd@La-BDC MOF nanocomposite in catalysis, gas storage, and separation technologies. The unique 2D sheet-like morphology can enhance the specific surface area and the accessibility of the active sites,[26,27] while the polycrystalline structure may affect the material's mechanical properties and thermal stability,[28] making it a promising candidate for advanced functional materials.

3.1.5. Brunauer–Emmett–Teller (BET) studies. Investigations with N_2 adsorption–desorption showed that the Pd@La-BDC MOF is porous (Fig. 5). According to the International Union of Pure and Applied Chemistry (IUPAC) analysis, the isotherm observed closely resembles a type IV adsorption isotherm,

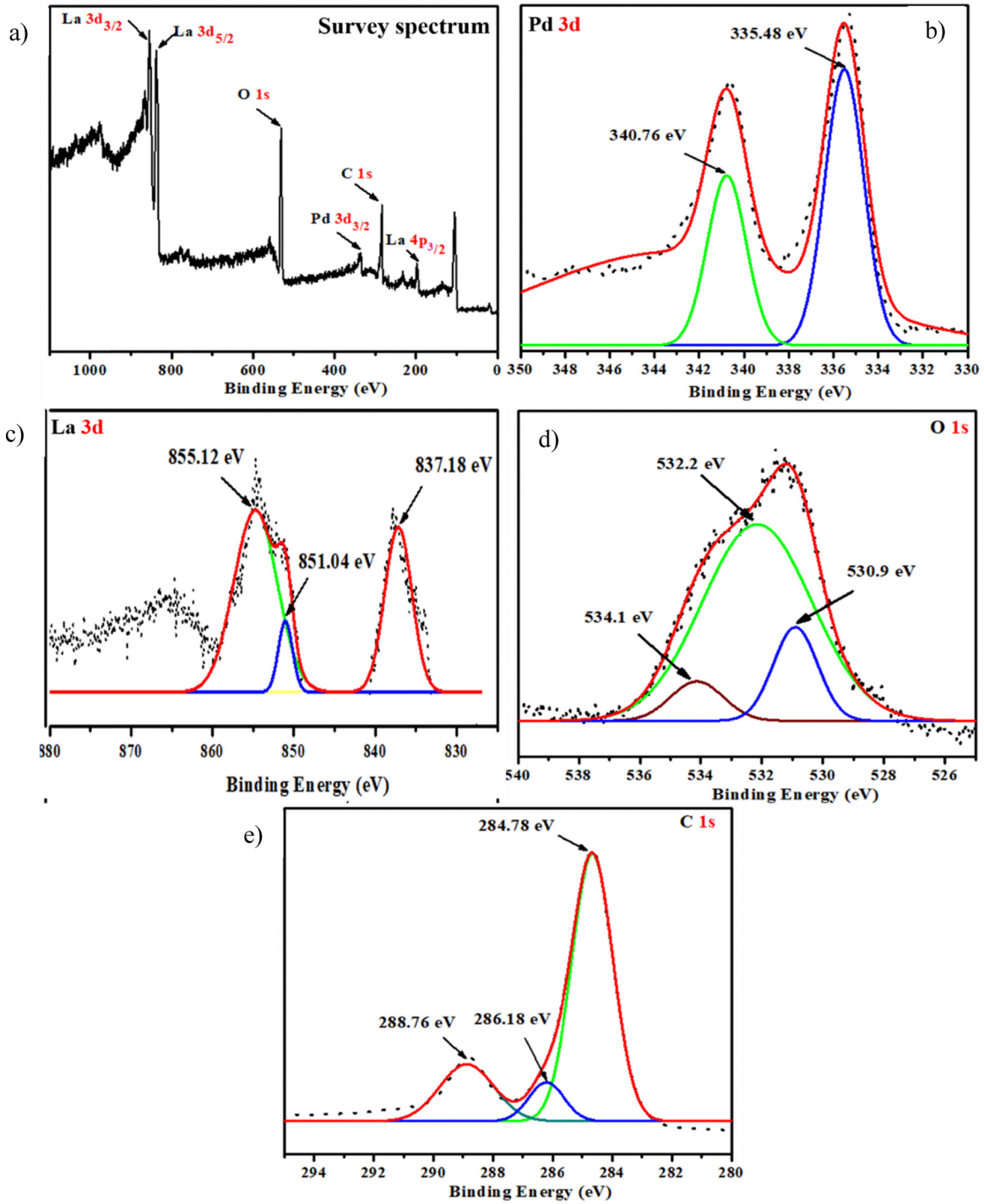

Fig. 6 (a) Survey Spectrum; (b–e) XPS spectra of all constituent elements in the Pd@La-BDC MOF nanocomposite, revealing the detailed elemental composition and oxidation states within the material.

indicative of mesoporous materials. The Brunauer–Emmett–Teller (BET) analysis measured a micropore volume of 0.00376523 $cm^3\ g^{-1}$, a total pore volume of 0.1256 $cm^3\ g^{-1}$, and a specific surface area of 368.14 $m^2\ g^{-1}$ (Fig. 5b). These results highlight the potential of the Pd@La-BDC MOF for various applications, particularly due to its high specific surface area and the presence of both micro- and mesopores. Whereas, for the La-BDC MOF, the micropore volume, total pore volume, and specific surface area are 0.0033463 $cm^3\ g^{-1}$, 0.1065 $cm^3\ g^{-1}$, and 321.31 $m^2\ g^{-1}$, respectively (Fig. 5a). Such characteristics are crucial for enhancing the material's adsorption capacity and catalytic efficiency.[29,30]

3.1.6. X-ray photoelectron spectroscopy (XPS). The synthesized materials' elemental states were investigated using XPS (Fig. 6). According to the survey spectrum of the Pd@La-BDC MOF nanocomposite (Fig. 6), the surface contains Pd, La, C, and O. The Pd@La-MOF nanocomposite's surface components and associated electronic states were examined using the XPS technique. Fig. 6a shows the survey spectrum of the Pd@La-MOF nanocomposite, which reveals the existence of elements like Pd, La, O and C. The Pd@La-MOF nanocomposite's Pd 3d spectra were deconvoluted into two central binding energies at 340.76 eV and 335.48 eV, which coincide with the peaks of Pd^0 and Pd^{2+} species, respectively, according to subsequent Pd 3d investigation.[30] The La 3d spectrum shows three separate peaks *viz.* 837.98, 851.84, and 855.12 eV, which correspond to La $3d_{1/2}$ and La $3d_{3/2}$, respectively. For C 1s the peaks at 284.78 eV, 286.18 eV and 288.76 eV are attributed to graphitic, alcoholic, and carboxyl carbons, correspondingly.[31] For O 1s, the peak at 530.9 eV, 532.2 eV and 534.2 eV are attributed to metallic oxygen (La–O), hydroxyl groups and O═C═O bonding, respectively.[32]

3.1.7. Thermogravimetric analysis. Examining the MOF's thermal stability before using it in the alkylation reaction of amines was another crucial task. The TGA run of Pd@La-BDC MOF was monitored from room temperature to 900 °C. In the TGA curve (Fig. 7), a loss of only 8% was observed when heated up to 200 °C, which could be due to loss of unbound water trapped in the porous framework of the MOF. Thereafter, 10–11% weight loss could only be recorded from 250 °C to 580 °C; and a sharp decline beyond 580 °C showed the degradation of the MOF under study. Thus, it can be concluded from TGA studies that the synthesized MOF was found to be stable in the experimental range of amine alkylation.

3.2. Catalytic evaluation

To start with assessment of the catalytic efficacy of the synthesized MOFs in the *N*-alkylation of amines, firstly aniline, chosen as a model amine substrate, was treated with benzyl alcohol at 150 °C in toluene as a solvent (Scheme 2). The reaction was carried out both with and without the La-BDC MOF and Pd@La-BDC MOF catalyst and the percentage conversion of the reactant achieved in each case was evaluated using GC-FID experiments using *n*-hexadecane as an internal standard and the results are reported in Table 1.

Notably, no product formation took place when the reaction was performed in the absence of the MOF catalyst (Table 1, entry 1) even after 6 h, and only 61% substrate conversion took place in an interval of 6 h, when the same reaction was carried out with 5 mol% of La-BDC MOF (Table 1, entry 2). To our surprise, upon replacing the La-BDC MOF with Pd@La-BDC MOF in the same reaction, the % conversion of aniline was found to enhance to 94% (Table 1, entry 4). Thus, integrating Pd into the La-BDC MOF catalyst was proven to improve the

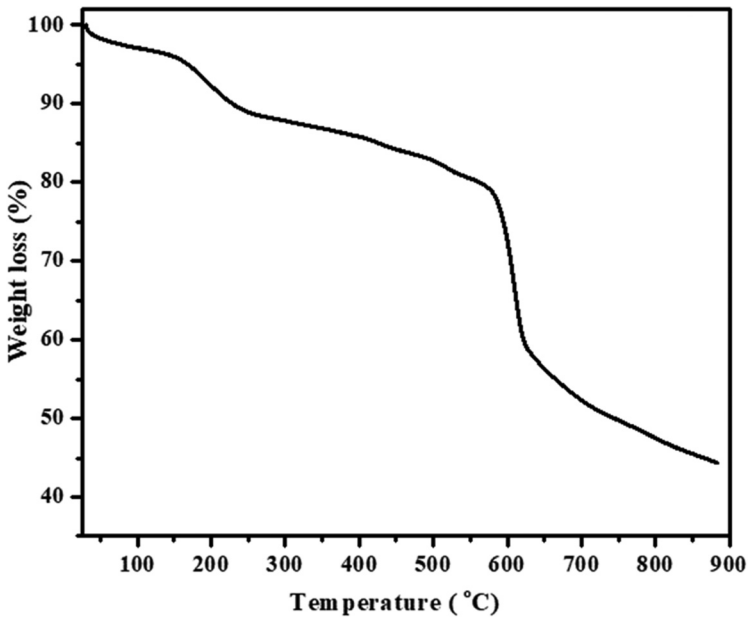

Fig. 7 Thermogravimetric analysis (TGA) of the Pd@La-BDC MOF nanocomposite shows a slight weight loss after 250 °C, followed by significant degradation at 580 °C.

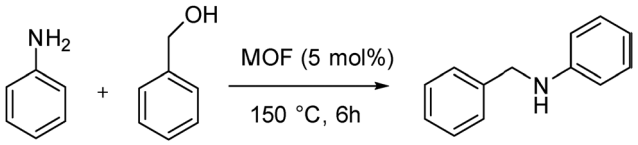

Scheme 2 Reaction of aniline with benzyl alcohol in the catalytic presence of La-BDC and Pd@La-BDC MOFs.

Table 1 Optimization of the conditions for the reaction of aniline with benzyl alcohol

Entry	Catalyst	Base (equiv.)	Solvent	% conversion
1	No catalyst	—	—	Nil
2	La-BDC MOF	—	Toluene	61
3	Pd@La-BDC MOF	—	Toluene	94
4	Pd@La-BDC MOF	KOH (2)	Toluene	89
5	Pd@La-BDC MOF	KOH (5)	Toluene	92
6	Pd@La-BDC MOF	NaOH (2)	Toluene	89
7	Pd@La-BDC MOF	NaOH (5)	Toluene	91
8	Pd@La-BDC MOF	KO^{t}Bu (2)	Toluene	91
9	Pd@La-BDC MOF	KO^{t}Bu (5)	Toluene	95
10	Pd@La-BDC MOF	$(C_2H_5)_3N$ (2)	Toluene	83
11	Pd@La-BDC MOF	$(C_2H_5)_3N$ (5)	Toluene	85
12	Pd@La-BDC MOF	—	Hexane	91
13	Pd@La-BDC MOF	—	Xylene	87
14	Pd@La-BDC MOF	—	THF	77
15	Pd@La-BDC MOF	—	DMF	72

General reaction conditions: aniline 10 mmol, benzyl alcohol 50 mmol, catalyst 5 mol%, 150 °C, 6 h; conversion and selectivity percentage were determined by GC-FID using hexadecane as an internal standard.

yields for the reaction product, possibly due to greater H-borrowing tendency of the La from the substrate as explained in H-borrowing methodology explained in the later section under mechanistic studies.

3.2.1. Solvent effects and effect of adding external base. Selecting aniline as a model amine substrate and Pd@La-BDC MOF as a model catalyst, a series of run experiments were carried out to check the effect of the addition of various bases and solvents on the benzylation of aniline. Interestingly, the addition of 2 to 5 equiv. of KOH, NaOH, KO^{t}Bu and $(C_2H_5)_3N$ bases had little or no effect onto the % conversion of the substrate as can be seen from entries 4–11, Table 1. On a similar note, the replacement of toluene with hexane, xylene, THF or DMF lead to poor % conversion values in comparison to that in toluene (entries 12–15, Table 1), which may be due to the polar nature of the THF and DMF.

3.2.2. Reaction condition optimization. Following an analysis of how solvent choice and the addition of external bases affected the % conversion of the reactants and thus yields of the product, the reaction conditions were further optimized to improve the yields of the product further, by recording the percentage conversion of reactant with alteration in the molar ratio of reactants, the catalytic loading of Pd@La-BDC MOF and the reaction temperature.

3.2.3. Effect of temperature. As per the H-borrowing mechanism depicted in Scheme 1, the alcohol substrate is firstly oxidised to an aldehyde, which condenses with the amine substrate to form an imine intermediate, that finally borrows back hydrogen to deliver an alkylated amine as the product. The reaction temperature has been found to play a critical role in this, as the percentage isolation of imine (**1**) and alkylated products (**2**) has been found to be a function of reaction temperature.[15,18] To establish the same in the present case, the reaction mixture was analysed for the percentage isolation of benzaldehyde, imine (**1**) and alkylated amine substrates (**2**) (Scheme 3) using GCMS, and the yields of each of these were plotted as a function of temperature (Fig. 8a).

It was observed that at lower temperatures of 90–120 °C, the yields of the alkylated product (**2**) were low in comparison to the imine product (**1**) (Fig. 8a). But an increase in temperature beyond 120 °C increased the selectivity towards the amine product (**2**) and at 150 °C a maximum selectively of 97% towards the amine product was achieved (Fig. 8a).

3.2.4. Effect of reactant molar ratio and catalytic dosage. After optimizing the temperature conditions, the relative percentages of the imine (**1**) and alkylated amine (**2**) products were measured as a function of variation in reactant molar ratio and the amount of catalyst fed and the results are plotted in Fig. 8b and c. Among the various reactant ratios tested (Fig. 8b), when the aniline and benzyl alcohol were taken in a ratio 1 : 5 or greater, a selectivity of 97% was achieved for *N*-benzylaniline in an interval of 5 hours at 150 °C. Interestingly, no over-alkylated tertiary amine products were isolated under any conditions. The effect of catalytic dosage on the % conversion of substrate is shown in Fig. 8c. It is clear from Fig. 8c that a maximum conversion of 97% was achieved with 5 mol% of catalytic dosage in 5 h. Thus, a reactant ratio of 1 : 5, catalytic dosage of 5 mol%, and temperature of 150 °C were selected for further exploring the substrate scope.

3.2.5. Kinetics of the reaction. The mechanism of the reaction following the H-borrowing pathway, in general, if presented step by step, can be outlined as in Scheme 4. Eqn (1) involves dehydrogenation of benzyl alcohol by the abstraction of a hydrogen by the Pd@La-BDC MOF catalyst

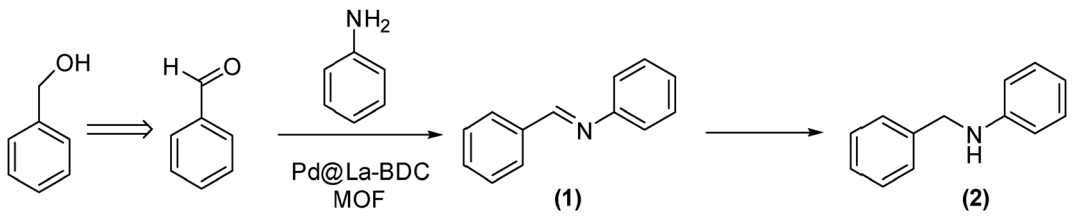

Scheme 3 H-borrowing reaction pathway for *N*-benzylation of aniline in the catalytic presence of Pd@La-BDC MOF.

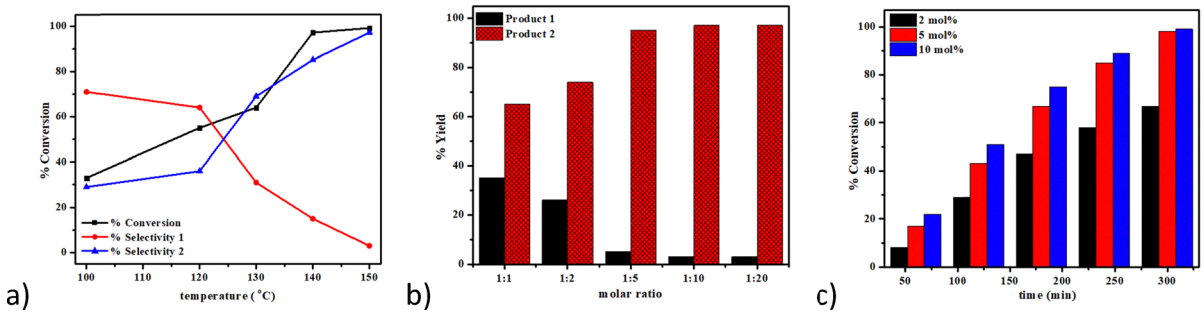

Fig. 8 Optimization of the reaction conditions for the Pd@La-BDC MOF-catalyzed *N*-benzylation reaction: (a) effect of temperature variation; (b) influence of varying molar ratios of reactants (aniline : benzyl alcohol); and (c) impact of different catalytic dosages.

$$PhCH_2OH + Pd@La\text{-}BDC\ MOF \xrightarrow{K_a} PhCHO + Pd@La\text{-}BDC\ MOF.2H \quad \textbf{(Eqn-1)}$$

$$PhCHOH + RNH_2 \xrightarrow{K_b} PhCH{=}NR \quad \textbf{(Eqn-2)}$$

$$PhCH{=}NR + Pd@La\text{-}BDC\ MOF.2H \xrightarrow{K_c} PhCH_2\text{-}NHR + Pd@La\text{-}BDC\ MOF \quad \textbf{(Eqn-3)}$$

Scheme 4 The step-wise general H-borrowing mechanism of alkylation of amines with benzyl alcohol.

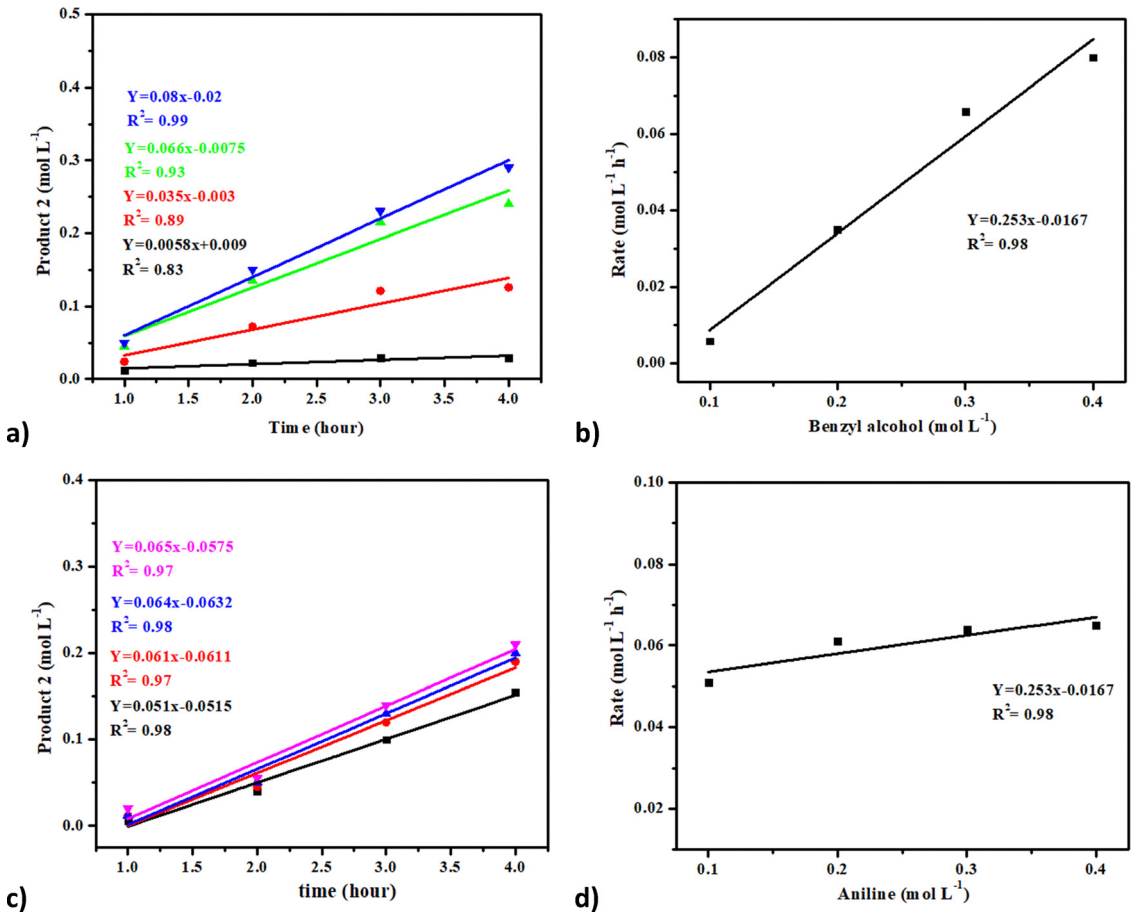

Fig. 9 Kinetics of the reaction: (a) amount of product as a function of benzyl alcohol conc.; (b) reaction order w.r.t. benzyl alcohol conc.; (c) amount of product as a function of aniline conc.; (d) reaction order w.r.t. aniline conc.

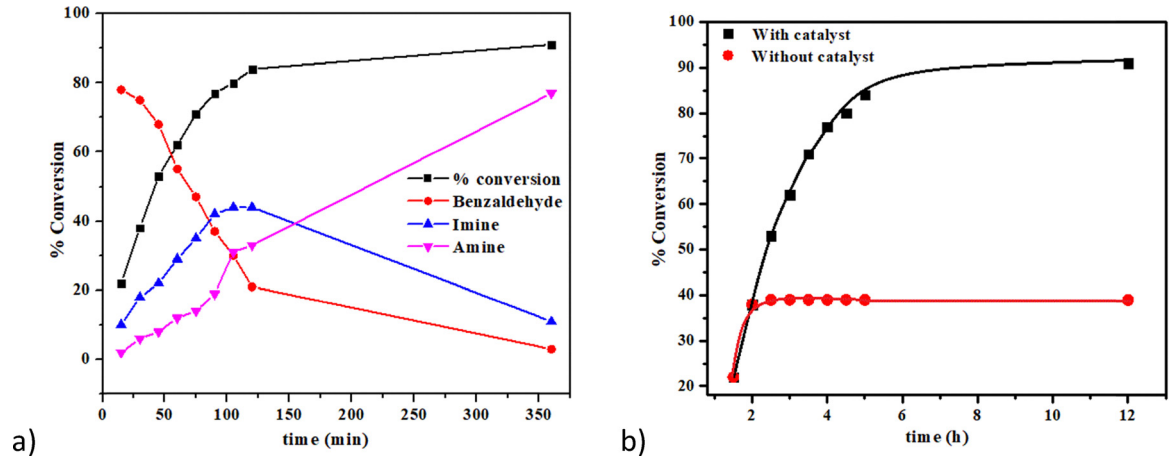

Fig. 10 (a) Percentage conversion for the substrate, intermediates and amines during the course of the reaction; (b) hot filtration tests; 10 mmol aniline, 5 mol% Pd@La-BDC, 150 °C.

forming benzaldehyde and the hydrogenated Pd@La-BDC MOF complex. Eqn (2) represents the condensation among benzaldehyde and the amine substrate leading to imine formation. And in the last equation the hydrogenated Pd@La-BDC MOF complex returns a hydrogen to the imine generating an alkylated amine as the final product.

To determine the overall kinetics of the reaction, the amount of one of the reactants out of aniline and benzyl alcohol was varied (0.2–0.8 mol) while that of the other was kept constant at 0.4 mol and the results are plotted in Fig. 9. The initial reaction rates were determined in both cases. The reaction rates were then plotted against the conc. of the reactant under consideration (Fig. 9c and d). The rate of the reaction varied linearly with conc. of benzaldehyde, while it was found to be independent of the aniline concentration. Thus, the rate of the reaction can be considered first order w.r.t. benzyl alcohol and thus the formation of benzaldehyde is the rate limiting step in the present case, which is in agreement with previous reports.[15,33]

3.3. Hydrogen borrowing mechanism

The *N*-alkylation of amines in the catalytic presence of transition metal-based catalysts has been reported to follow the H-borrowing pathway,[14] wherein the transition metal is involved in the exchange of hydrogen with the substrate as depicted in Schemes 1 and 4. In order to establish the same in the present case, the reaction mixture was monitored over a period of time and the % conversion for substrate, intermediates and product were plotted against time (Fig. 10). The reaction profile (Fig. 10) showed that benzaldehyde pre-formed in larger quantities declined with the passage of time and the amount of another intermediate imine increased in a slow fashion in the initial phase and began to decline after an interval of 2 h. At the end of the reaction, *i.e.* after 6 h, the alkylated amine was the major product, with little or no imine and aldehyde substrate.

Additionally, hot filtration tests were carried out to verify that the reaction ceases after the catalyst is removed from the reaction mixture. The hot reaction mixture was filtered after an interval of 2 h to separate the catalyst and the remaining solution was subjected to similar conditions of temperature. No further changes were observed in the percentage conversion (Fig. 10b), showing that the reaction ceased after elimination of the catalyst from the reaction mixture.

Based on the results in Fig. 10a, the plausible reaction mechanism can be outlined as in Scheme 5. The reaction begins with the deprotonation of benzyl alcohol by the metallic cluster on the Pd@La-BDC MOF, resulting in the formation of a benzaldehyde molecule and the generation of Pd-hydride species. The formed benzaldehyde molecule adsorbs onto the Pd site, which increases its electrophilicity and, consequently, its reactivity. This activated benzaldehyde molecule becomes more susceptible to nucleophilic attack by the amine substrate, generating an imine intermediate, and in the process, a water molecule is eliminated. Subsequently, the Pd-hydride species generated in the first step comes into play. It hydrogenates the imine group, reducing it to a secondary amine product.

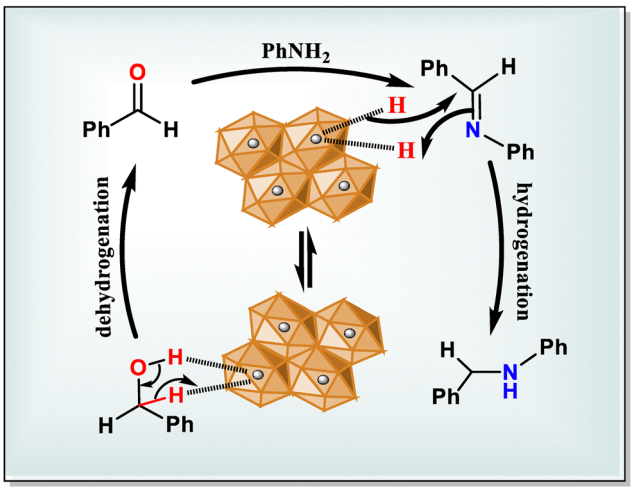

Scheme 5 H-borrowing mechanism for the Pd@La-BDC MOF-mediated *N*-alkylation reaction, illustrating the key steps and intermediate species involved in the catalytic process.

Table 2 *N*-Benzylation of various aromatic amines with benzyl alcohol in the presence of Pd@La-BDC MOF

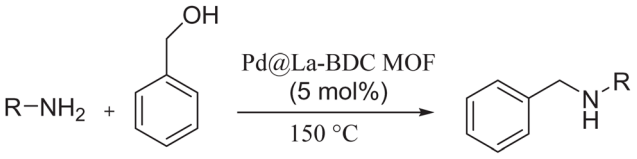

(3) (4) (5)

S. no.	Reactant (3)	Product (5)	Duration (in hours)	% yield
1	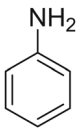	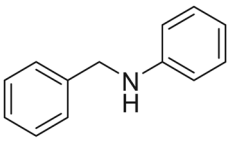 **(5a)** [14]	4	94
2	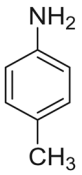	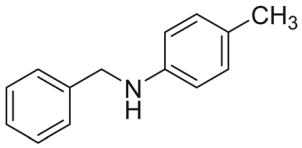 **(5b)** [34]	4	92
3	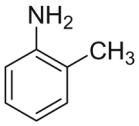	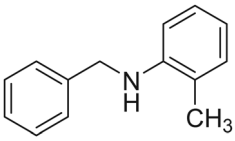 **(5c)** [34]	4	90
4	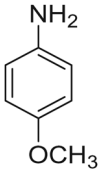	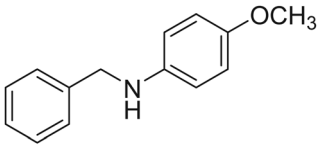 **(5d)** [10,15]	4.5	91
5	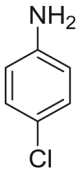	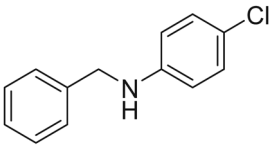 **(5e)** [10,15]	6	79
6	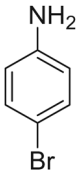	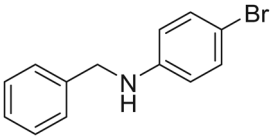 **(5f)** [15]	6	76
7	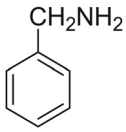	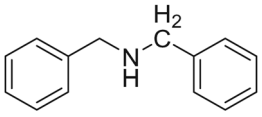 **(5g)** [11]	4	91
8	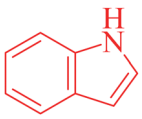	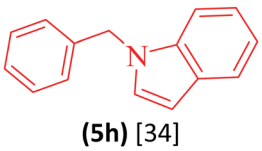 **(5h)** [34]	6	87

Table 2 (*continued*)

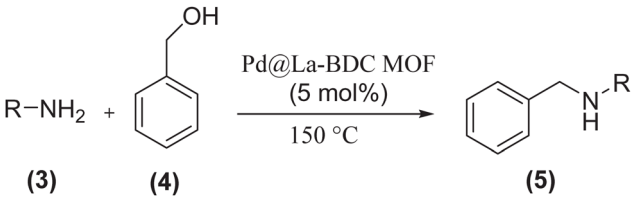

(3) (4) (5)

S. no.	Reactant (3)	Product (5)	Duration (in hours)	% yield
9	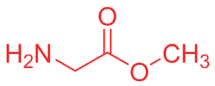	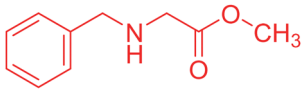 **(5i)** [35]	6	85

General reaction conditions: aniline 10 mmol, benzyl alcohol 50 mmol, catalyst 5 mol%, 150 °C.

The active site on the Pd@La-BDC MOF is regenerated during the final step, making it available for subsequent catalytic cycles.

3.3.1. Substrate scope of Pd@La-BDC MOF-catalysed *N*-benzylation. With the optimized reaction conditions in hand and after establishing the mechanism involved, the current approach was extended to *N*-benzylate differently substituted amines with benzyl alcohol in the presence of 5 mol% of the Pd@Al-BDC MOF catalyst. The alkylation reactions were carried out with various amine substrates and the results are listed in Table 2.

The results in Table 2 showed that all the examined aromatic amines could be converted into their corresponding *N*-benzylated products during the alkylation reactions, albeit the yields varied. The chloro and bromo derivatives of aniline delivered products in slightly lower yields (Table 2, entries 5 and 6), while the yields of *N*-benzylation products were higher with electron rich anilines, *i.e.* *o*-toluidine, *p*-toluidine and anisidine. Furthermore, indole and methyl glycinate were also subjected to alkylation under similar experimental conditions, and in both cases, yields of 87% and 85% were recorded for the corresponding *N*-alkylated products (Table 2, entries 8 and 9). Thus, the present methodology served to benzylate a diverse array of amine substrates under high to excellent yields.

3.4. Catalytic reusability

A crucial component of heterogeneous catalysis is the catalyst's capacity for reuse. To evaluate this, the heterogenous MOF catalyst separated at the end of the reaction was washed with a water–ethanol mixture to get rid of reactants adhered to its surface. Later, it was dried by keeping it in an oven at 150 °C for 2 h, and then used for the subsequent run. Upon re-using the same catalyst five times, only a meagre drop in catalytic action was noticed (Fig. 11a). The XRD patterns of the catalyst retrieved after the fifth run were recorded to look for any modifications that might have happened during the course of the reaction (Fig. 11b). Notably, the XRD pattern showed no additional peaks w.r.t. the XRD patterns of the original MOF catalyst. Thus, it can be generalized that the catalyst remained stable during the reaction and is reusable.

3.5. Comparative analysis with existing literature

The outcomes of the present work have been compared with those obtained in the presence of other transition metal-based heterogenous catalysts. Upon comparison with the literature reports provided in Table 3, it can be figured out that the

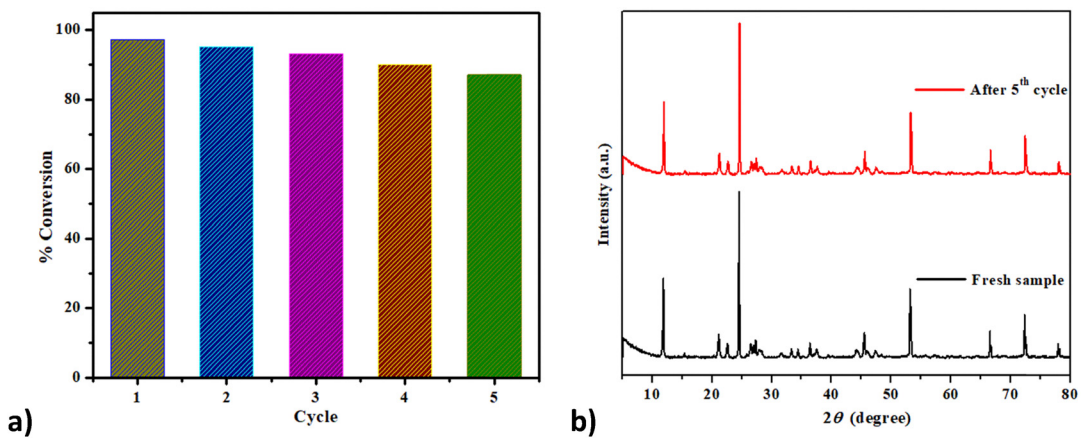

Fig. 11 (a) Graph showing catalytic reuse of the Pd@La-BDC MOF, highlighting its stability and reusability over multiple cycles; (b) X-ray diffraction patterns of fresh and recovered MOF samples, demonstrating the retention of structural integrity after catalysis.

Table 3 Comparative account of MOF catalyzed *N*-alkylation of amines

Entry	Catalyst	Reaction conditions	Alkylation source	Alkylated product (% yield)	Ref.	Advantages/disadvantages
1	Cu-Fe(3)HT-300	163 °C, 24 h	Benzyl alcohol	88	14	Low substrate ratio, longer duration, byproducts
2	TiOH-80	180 °C, 15–96 h	Alcohols	90–97	36	Wide substrate scope, longer duration, byproduct
3	$MnBr(CO)_5$	130 °C, 20 h	Alcohols	29–92	10	Wide substrate scope, base requirement, longer duration
4	Hf-MOF-808	120–140 °C, 3–23 h	Benzyl alcohol	70–90	15	Low temp., low yields, longer duration
5	UiO66-NH_2-[LIr]BF_4	80–180 °C, 2–24 h	Benzyl alcohol	90–100	37	High yields, wide substrate scope, longer duration
6	Pd@La-BDC MOF	150 °C, 4–6 h	Benzyl alcohol	79–94	Present work	Short duration, high selectivity

Pd@La-BDC MOF catalyst utilized for *N*-benzylation in the present investigation performs on par with the results obtained with already reported MOF catalysts. A higher alkylation percentage has been obtained in the present case under less drastic conditions of temperature (entries 1 and 6, Table 3). Moreover, a number of amine substrates could be selectively converted to the corresponding mono *N*-methylated products under the optimized reaction conditions. The heterogenous catalyst was easily retrieved at the end of the reaction and the reusability of the heterogenous catalyst has also been established (Fig. 11).

4. Conclusion

This study successfully synthesized and utilized a Pd-incorporated La-BDC MOF catalyst for the *N*-benzylation of amines, employing a solvothermal method and *in situ* reduction of the Pd precursor with $NaBH_4$. The resulting Pd-doped La-BDC MOF composite demonstrated a high surface area of 368.14 $m^2\ g^{-1}$ and pore volume of 0.1256 $cm^3\ g^{-1}$ with a microporous structure (micropore volume of 0.00376523 $cm^3\ g^{-1}$) that significantly enhanced its catalytic performance. The catalyst achieved a maximum selectivity of 97% under the optimized conditions, efficiently benzylating various amine substrates including electron poor aromatic amines and amino acid esters. The isolation of imine and benzaldehyde intermediates during the time-monitored reaction profile confirmed that the reaction followed a hydrogen auto-transfer pathway. The robustness and practical utility of the Pd@La-BDC MOF catalyst were further validated through reusability and hot filtration tests, underscoring its potential as a reliable heterogeneous catalyst for *N*-benzylation reactions.

Author contributions

Amreet Kaur: experimental and writing original draft; Dr Sandeep Kaushal: conceptualization, characterization and formal analysis; Dr Rahul Badru: conceptualization, methodology, draft revision and supervision; Dr Yadvinder Singh & Dr Avatar Singh: validation, reviewing and editing.

Conflicts of interest

There are no conflicts to declare.

Data availability

The data supporting this article have been included as part of the ESI.†

Acknowledgements

The authors acknowledge SGGSWU, Fatehgarh Sahib for providing the necessary laboratory facilities. They are also thankful to SAIF Lab at Panjab University, Chandigarh, and Punjabi University, Patiala, for spectral analysis.

References

1 G. Fiorani, A. Perosa and M. Selva, Dimethyl carbonate: a versatile reagent for a sustainable valorization of renewables, *Green Chem.*, 2018, **20**, 288–322.
2 A. Corma, J. Navas and M. J. Sabater, Advances in One-Pot Synthesis through Borrowing Hydrogen Catalysis, *Chem. Rev.*, 2018, **118**(4), 1410–1459.
3 B. G. Reed-Berendt, D. E. Latham, M. B. Dambatta and L. C. Morrill, Borrowing Hydrogen for Organic Synthesis, *ACS Cent. Sci.*, 2021, **7**(4), 570–585.
4 P. Tundo and M. Selva, The Chemistry of Dimethyl Carbonate, *Acc. Chem. Res.*, 2002, **35**(9), 706–716.
5 P. Tundo, M. Musolino and F. Arico, The reactions of dimethyl carbonate and its derivatives, *Green Chem.*, 2018, **20**, 28–85.
6 S. Bera, L. M. Kabadwal and D. Banerjee, Harnessing alcohols as sustainable reagents for late-stage functionalisation: synthesis of drugs and bio-inspired compounds, *Chem. Soc. Rev.*, 2024, **53**, 4607–4647.
7 G. Sivakumar, R. Kumar and V. Yadav, *et al.*, Multi-Functionality of Methanol in Sustainable Catalysis: Beyond Methanol Economy, *ACS Catal.*, 2023, **13**(22), 15013–15053.
8 S. M. Khake and N. Chatani, Rhodium(III)-catalyzed oxidative C-H alkylation of aniline derivatives with allylic alcohols

to produce β-Aryl Ketones, *ACS Catal.*, 2022, **12**(8), 4394–4401.
9 K. O. Marichev and J. M. Takacs, Ruthenium-catalyzed amination of secondary alcohols using borrowing hydrogen methodology, *ACS Catal.*, 2016, **6**, 2205–2210.
10 V. G. Landge, A. Mondal and V. Kumar, *et al.*, Manganese catalyzed N-alkylation of anilines with alcohols: ligand enabled selectivity, *Org. Biomol. Chem.*, 2018, **16**, 8175–8180.
11 Z. Ma, B. Zhou and R. G. Kadam, *et al.*, Reusable Co-nanoparticles for general and selective N-alkylation of amines and ammonia with alcohols, *Chem. Sci.*, 2022, **13**, 111–117.
12 T. T. Dang, B. Ramalingam, S. P. Shan and A. M. Seayad, An efficient Palladium-catalyzed N-alkylation of amines using primary and secondary alcohols, *ACS Catal.*, 2013, **3**, 2536–2540.
13 G. S. Lu, Z. L. Ruan and Y. Wang, *et al.*, Catalytic Reductive Amination and Tandem Amination–Alkylation of Esters Enabled by a Cationic Iridium Complex, *Angew. Chem., Int. Ed.*, 2025, **64**(12), e202422742.
14 W. S. Putro, T. Hara, N. Ichikuni and S. Shimazu, One-pot synthesis of aniline N-alkylation from benzyl alcohol over Cu-Fe catalyst, *Appl. Catal., A*, 2020, **602**, 117519.
15 B. Bohigues, S. Rojas-Buzo, M. Moliner and A. Corma, Coordinatively unsaturated Hf-MOF-808 prepared via hydrothermal synthesis as a bifunctional catalyst for the tandem N-alkylation of amines with benzyl alcohol, *ACS Sustainable Chem. Eng.*, 2021, **9**(47), 15793–15806.
16 Y. Lu, H. Chai and K. Yu, *et al.*, A reusable MOF supported single-site nickel-catalyzed direct N-alkylation of anilines with alcohols, *Tetrahedron*, 2022, **124**, 132993.
17 X. Wang, T. Li and H. Wang, *et al.*, Identifying active sites at the Cu/Ce interface for hydrogen borrowing reactions, *J. Catal.*, 2023, **418**, 163–177.
18 T. Tong, M. Douthwaite and L. Chen, *et al.*, Uncovering structure-activity relationships in Pt/CeO_2 catalysts for Hydrogen-borrowing amination, *ACS Catal.*, 2023, **13**(2), 1207–1220.
19 A. Sharma, S. Bedi and K. Verma, *et al.*, Ce-Zr UiO-66 MOF as recyclable heterogeneous catalyst for selective N-methylation, *Polyhedron*, 2023, **242**, 116517.
20 A. Sharma, K. Verma, S. Kaushal and R. Badru, A novel 2-D accordion like Al-BPED MOF as reusable and selective catalyst for N-alkylation of amines with dialkylcarbonates, *Appl. Organomet. Chem.*, 2022, **36**(11), e6814.
21 A. Sharma, K. Verma, S. Kaushal and R. Badru, Selective N-alkylation of amines with DMC over biogenic Cu-Zr bimetallic nanoparticles, *ACS Omega*, 2021, **6**, 15300–15307.
22 M. Kaur, A. Sharma and Y. Singh, *et al.*, Pd supported Al-BDC MOF for efficient and selective N-methylation of amines under solventless conditions, *Emergent Mater.*, 2024, **7**, 1683–1693.
23 M. Sharma, K. Verma and A. Kaushik, *et al.*, DBU-MIm coupled ionic liquids as reusable catalysts for the Biginelli reaction, *Mol. Catal.*, 2023, **536**, 112906.
24 M. Govarthanan, C. Jeon and W. Kim, Synthesis and characterization of Lanthanum-based metal organic framework decorated polyaniline for effective adsorption of lead ions from aqueous solutions, *Environ. Pollut.*, 2022, **303**, 119049.
25 Q. Wu, C. Shen and C. Liu, Amino acid (histidine) modified Pd/SiO_2 catalyst with high activity for selective hydrogenation of acetylene, *Appl. Surf. Sci.*, 2023, **607**, 154976.
26 Y. Zhang, K. Nie and L. Yi, *et al.*, Recent Advances in Engineering of 2D Materials-Based Heterostructures for Electrochemical Energy Conversion, *Adv. Sci.*, 2023, **10**(31), e2302301.
27 B. Chettiannan, G. Arumugam and M. Selvaraj, R. Rajendran. Exploring the effect of morphology on electrochemical performance of nickel and cobalt metal-organic frameworks and their derivatives for supercapacitor and hydrogen evolution, *J. Energy Storage*, 2024, **94**, 112390.
28 W. Hao, C. Sui and G. Cheng, *et al.*, High-Strength Polycrystalline Covalent Organic Framework with Abnormal Thermal Transport Insensitive to Grain Boundary, *Nano Lett.*, 2024, **24**(14), 4248–4255.
29 T. Shi, Z. Wu and Z. Wu, *et al.*, Postsynthetic amine modification of porous organic polymers for CO_2 capture and separation, *J. Polym. Sci.*, 2024, **62**(8), 1554.
30 X. Hu, J. Wang and S. Li, *et al.*, Pd-doped HKUST-1 MOFs for enhanced hydrogen storage: effect of hydrogen spillover, *RSC Adv.*, 2023, **13**, 14980–14990.
31 C. V. Ramana, R. S. Vemuri and V. V. Kaichev, *et al.*, X-ray Photoelectron Spectroscopy Depth Profiling of La_2O_3/Si thin films deposited by reactive magnetron sputtering, *ACS Appl. Mater. Interfaces*, 2011, **3**(11), 4370–4373.
32 M. F. Sunding, K. Hadidi and S. Diplas, *et al.*, XPS characterisation of in situ treated lanthanum oxide and hydroxide using tailored charge referencing and peak fitting procedures, *J. Electron Spectrosc. Relat. Phenom.*, 2011, **184**(7), 399–409.
33 S. Rojas-Buzo, P. Concepcion and A. Corma, *et al.*, *In Situ* generated active Hf-hydride in Zeolites for the tandem N-alkylation of amines with benzyl alcohol, *ACS Catal.*, 2021, **11**(13), 8049–8061.
34 N. Hofmann and K. C. Hultzsch, Switching the N-Alkylation of Arylamines with Benzyl Alcohols to Imine Formation Enables the One-Pot Synthesis of Enantioenriched α-N-Alkylaminophosphonates, *Eur. J. Org. Chem.*, 2019, 3105–3111.
35 S. Ghaffari and F. Kazemi, Highly Efficient Synthesis of N-Alkyl-α-amino Acid Methyl Esters by Microwave Irradiation, *ChemistrySelect*, 2021, **6**, 2901–2905.
36 F. Niu, Q. Wang and Z. Yan, *et al.*, Highly efficient and selective N-alkylation of amines with alcohols catalyzed by in situ rehydrated Titanium hydroxide, *ACS Catal.*, 2020, **10**(5), 3404–3414.
37 A. M. Rasero-Almansa, A. Corma, M. Iglesias and F. Sanchez, Design of a bifunctional Ir-Zr based metal-organic framework heterogeneous catalyst for the N-alkylation of amines with alcohols, *ChemCatChem*, 2014, **6**(6), 1794–1800.